DFT AND TD-DFT INVESTIGATION OF THE ELECTRONIC STRUCTURE, THERMODYNAMIC STABILITY, SPECTRAL PROPERTIES, AND REACTIVITY OF 3-(1,3-DIHYDROXYPROPAN-2-yl)BENZO[*d*]OXAZOL-2(3*H*)-ONE

Nodira Rakhimova,
Department of Chemistry, Urgench State University named after Abu Rayhan Biruni, Kh. Alimjan 14 h., Urgench, 220100, Uzbekistan.
Student
nodiraraximova067@gmail.com

Khushnudbek Eshchanov
Department of Chemistry, Urgench State University named after Abu Rayhan Biruni, Kh. Alimjan 14 h., Urgench, 220100, Uzbekistan.
PhD, associate professor.
xeshchanov77@gmail.com

Dilshod Dushamov
Department of Chemistry, Urgench State University named after Abu Rayhan Biruni, Kh. Alimjan 14 h., Urgench, 220100, Uzbekistan.
Associate professor.
dilshod.d71@mail.ru

ABSTRACT

In this work, the electronic structure, thermodynamic stability, and spectral properties of 3-(1,3-dihydroxypropan-2-yl)benzo[d]oxazol-2(3H)-one were investigated using DFT and TD-DFT methods at the B3LYP/6-311G(d,p) level in acetonitrile medium. Mulliken charge distribution analysis confirmed the nucleophilic character of the nitrogen atom and supported the SN2 reaction mechanism. HOMO–LUMO analysis revealed significant electron delocalisation and molecular stability with an energy gap of 8.09 eV. Molecular electrostatic potential (MEP), UV–Vis, and FTIR spectroscopy analyses demonstrated strong intramolecular charge transfer, polarisation of the carbonyl group, and the presence of characteristic functional groups. Thermodynamic calculations indicated that the reaction proceeds spontaneously within the studied temperature range.

Keywords: *Benzoxazolinone derivative, DFT calculations, HOMO–LUMO analysis, Mulliken charges, FTIR spectroscopy.*

INTRODUCTION

Heterocyclic compounds incorporating nitrogen and oxygen atoms play an important role in contemporary organic and medicinal chemistry because of their broad spectrum of biological effects and significant practical value [1, 2]. In particular, benzoxazolinone-based derivatives have attracted increasing scientific interest owing to their reported antimicrobial, antiinflammatory, antioxidant, and other pharmacologically relevant activities [3]. The physicochemical behaviour and chemical reactivity of these molecules are largely governed by the electronic distribution within the heterocyclic framework as well as the nature of the attached substituent groups.

In recent years, computational chemistry methods have become powerful tools for the detailed investigation of molecular geometry, electronic structure, thermodynamic stability, and possible reaction pathways with a high level of accuracy [4]. Among these approaches, Density Functional Theory (DFT) has been extensively applied to heterocyclic compounds due to its effectiveness in predicting electronic and structural characteristics, including molecular orbital energies, charge distribution, spectroscopic parameters, and intermolecular interactions [5,6]. Furthermore, analyses such as Mulliken atomic charges, frontier molecular orbitals (HOMO–LUMO), molecular electrostatic potential (MEP) surfaces, and theoretical spectral calculations are essential for interpreting the physicochemical and reactive properties of biologically active molecules [7].

N-alkylation of benzoxazolinone derivatives represents an important transformation in synthetic organic chemistry, since it enables structural modification of the heterocyclic framework and may considerably alter the biological activity of the resulting compounds [8]. In this context, the interaction of benzoxazolinone with 2-chloropropane-1,3-diol occurs via a nucleophilic substitution path-way, yielding 3-(1,3-dihydroxypropan-2-yl)benzo[*d*]oxazol-2(3*H*)-one as the target product [9]. The course of this reaction and the stability of the obtained compound are strongly affected by several factors, including the electron density on the nitrogen atom, the polarization of the C–Cl bond, and the influence of the reaction medium or solvent environment [10].

In the present work, the electronic structure and thermodynamic behaviour of 3-(1,3-dihydroxypropan-2-yl)benzo[*d*]oxazol-2(3*H*)-one were examined by means of DFT and TD-DFT approaches employing the B3LYP/6-311G(d,p) method together with the CPCM solvation model in acetonitrile solution [11]. Particular emphasis was placed on the evaluation of Mulliken atomic charges, Gibbs free energy changes, frontier molecular orbital (HOMO–LUMO) parameters, UV–Vis absorption

properties, molecular electrostatic potential (MEP) distribution, and FTIR spectral features [12]. The computational findings offer comprehensive insight into the reaction pathway, electron delocalisation effects, structural stability, and spectroscopic properties of the synthesised benzoxazolinone-based compound.

MATERIALS AND COMPUTATIONAL METHODS

A quantum-chemical study of 3-(1,3-dihydroxypropan-2-yl)benzo[*d*]oxazol-2(3*H*)-one was performed within the framework of Density Functional Theory (DFT). The target compound was synthesised via N-alkylation of benzoxazolinone with 2-chloropropane-1,3-diol in an acetonitrile medium, and its reaction pathway, together with electronic characteristics, was investigated theoretically.

All computational calculations were carried out using the Gaussian 09 program package. The initial molecular structure was generated and subsequently optimised without imposing any symmetry restrictions at the B3LYP/6-311G(d,p) level of theory. The B3LYP hybrid functional was employed because of its proven suitability for predicting the electronic and spectroscopic properties of heterocyclic organic systems with good accuracy. The 6-311G(d,p) basis set was chosen to achieve reliable geometric and electronic descriptors of the studied molecule.

In order to reproduce experimental conditions more realistically, solvent effects were taken into account using the CPCM (Conductor-like Polarizable Continuum Model), with acetonitrile selected as the solvent environment. The use of acetonitrile is particularly appropriate because its polar aprotic character facilitates SN2 nucleophilic substitution processes and contributes to the stabilisation of charged intermediates during the reaction.

Vibrational frequency calculations were carried out at the same theoretical level to verify that the optimized geometry represents a true minimum on the potential energy surface. The optimized structure exhibited no imaginary frequencies, indicating its geometric stability. In addition, thermodynamic quantities such as zero-point energy correction, thermal correction to energy, enthalpy, and Gibbs free energy were derived from the vibrational analysis.

Mulliken population analysis was applied to evaluate the electron density redistribution within the molecule and to identify possible nucleophilic and electrophilic active centers. The frontier molecular orbitals were also examined, including HOMO and LUMO energy values, the HOMO–LUMO energy separation, and intramolecular charge-transfer behavior. To further characterize reactive regions, molecular electrostatic potential (MEP) surfaces were generated, providing a visual representation of electron-rich and electron-deficient sites.

The electronic absorption spectrum was investigated using Time-Dependent Density Functional Theory (TD-DFT) at the same computational level. The calculated absorption bands and electronic transitions were analyzed with respect to π→π* and n→π* excita-tion processes. In parallel, theoretical FTIR spectra of the optimized structure were obtained to assign the characteristic vibrational modes associated with the functional groups of the molecule [13, 14].

Furthermore, the temperature dependence of Gibbs free energy was studied over the 298–400 K range. Linear relationships for both reactants and products were established to evaluate the thermodynamic feasibility and spontaneous nature of the reaction process.

RESULTS AND DISCUSSION

The results of the Mulliken charge distribution analysis made it possible to determine the redistribution of electron density during the reaction and to identify the nature of the reactive centres. According to the calculated data, a significant negative charge was observed on the nitrogen atom of the benzoxazolinone fragment ($q_N \approx -0.459$) (Figure 1). This result indicates that the nitrogen atom possesses a strong electron-donating character and actively participates in the reaction as a nucleophilic centre. Despite the resonance delocalisation of the lone electron pair of the nitrogen atom with the carbonyl group, sufficient electron density remains localised on the nitrogen atom, thereby creating favourable conditions for the N-alkylation reaction to proceed.

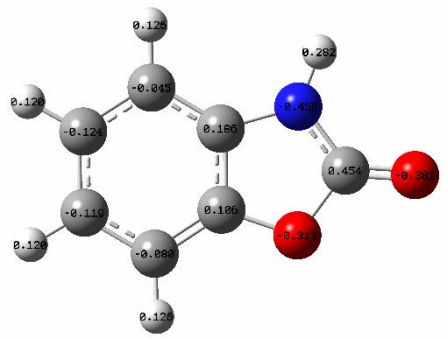

Fig. 1: Mulliken charge distribution map of 3-(1,3-dihydroxypropan-2-yl)benzo[*d*]oxazol-2(3*H*)-one

The pronounced negative charge localised on the carbonyl oxygen atom ($q_O \approx -0.381$) indicates strong polarisation within the C=O bond. Simultaneously, the considerable positive charge calculated for the carbonyl carbon atom ($q_C \approx +0.454$) reflects an amide-like electronic configuration in the heterocyclic system. Such electron density redistribution promotes effective conjugation throughout the molecule, thereby enhancing stabilisation of the heterocyclic framework.

Consequently, the delocalisation of electrons over the entire system contributes significantly to the thermodynamic stability and favourable formation of the final product.

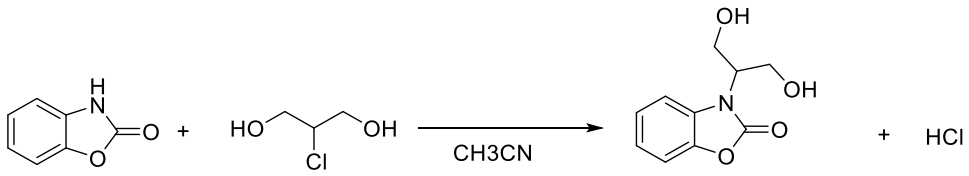

In the proposed reaction pathway, the polarisation of the C–Cl bond in the 2-chloropropane-1,3-diol molecule plays a crucial role in determining the reactivity of the substrate. Owing to the strong electronegativity of the chlorine atom, the bonded carbon atom ac-quires a partial positive charge, thereby forming an electrophilic centre susceptible to nucleophilic attack. The Mulliken charge anal-ysis clearly supports an SN2-type substitution mechanism, in which the electron-rich nitrogen atom attacks the electrophilic carbon centre. This process leads to the departure of the chloride ion and subsequent formation of the N-alkylated benzoxazolinone derivative (Figure 2).

The solvent environment also has a significant influence on the reaction progress. Acetonitrile, being a polar aprotic solvent, weakly solvates nucleophilic species and therefore preserves their high nucleophilic activity. As a consequence, the rate of bimolecular nucleophilic substitution reactions is enhanced considerably under these conditions. Thus, the selected solvent medium provides favourable conditions for efficient N-alkylation.

Furthermore, in the final product, electron density is delocalized over the carbonyl group, nitrogen atom, and aromatic heterocyclic framework, which contributes to additional stabilisation of the molecular structure. This extended conjugation increases the thermodynamic stability of the synthesised compound.

Overall, the Mulliken population analysis enabled the identification of both nucleophilic and electrophilic reactive centres partici-pating in the reaction and confirmed that the N-alkylation process follows an SN2 reaction pathway. The theoretical results are in good agreement with experimental observations and provide a clear explanation for the stability of the obtained product as well as the thermodynamically favourable and spontaneous character of the reaction.

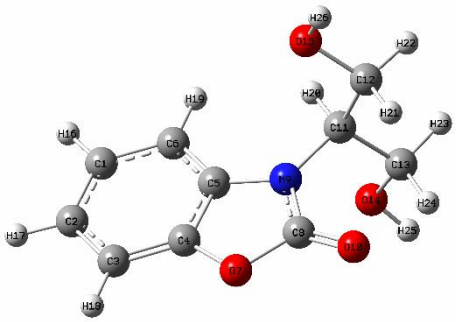

Fig. 2: Geometry-optimized structure of 3-(1,3-dihydroxypropan-2-yl)benzo[*d*]oxazol-2(3*H*)-one obtained at the B3LYP/6-311G(d,p) level.

The obtained computational data indicate that the studied molecule is both highly polarised and thermodynamically stable. The calculated dipole moment value of 4.0592 Debye reflects a pronounced asymmetry in electron density distribution and demonstrates the substantial influence of the heteroatoms on the molecular polarity. Such a relatively high polarity is expected to improve solubility in polar media and promote the formation of intermolecular hydrogen-bonding interactions. In addition, the negative Gibbs free energy value suggests that the compound possesses favourable thermodynamic stability and can exist as a stable molecular system under the investigated conditions (Table 1).

Table 1: Calculated thermodynamic and molecular parameters of 3-(1,3-dihydroxypropan-2-yl)benzo[*d*]oxazol-2(3*H*)-one

Parameters	Value
Molecular mass	209.06881 a.m.u
Dipole moment	4.0592 Debye
Zero-point correction	0.204180 Hartree
Thermal correction to Energy	0.217805 Hartree
Thermal correction to Enthalpy	0.218749 Hartree
Thermal correction to Gibbs Free Energy	0.162933 Hartree
Free Gibbs energy(G)	−743.387047 Hartree

The calculated Gibbs free energy functions for the reactants and products involved in the studied reaction are listed below (kJ/mol):

- benzoxazolinone: $G(T)\approx -1247088.8-0.3457T$
- 2-chloropropane-1,3-diol: $G(T)\approx -1914460.5-0.3581T$
- 3-(1,3-dihydroxypropan-2-yl)benzo[d]oxazol-2(3H)-one: $G(T)\approx -1951931-0.4916T$

- HCl: $G(T) \approx -1209868.3 - 0.1867T$

The obtained results show that, within the investigated temperature interval of 298–400 K, the Gibbs free energies of all considered species exhibit an approximately linear dependence on temperature with satisfactory correlation accuracy. Based on these linear approximations, the Gibbs free energy change for the overall reaction can be represented by the following expression (Figure 3): $\Delta G(T) \approx -250.0 + 0.0255T$.

The negative values of ΔG over the studied temperature range indicate that the reaction proceeds spontaneously under the investigated conditions. In addition, the relatively small temperature coefficient demonstrates that temperature variations have only a limited influence on the thermodynamic favorability of the process. These findings confirm that the formation of 3-(1,3-dihydroxypropan-2-yl)benzo[*d*]oxazol-2(3*H*)-one is thermodynamically favourable and results in a stable reaction product.

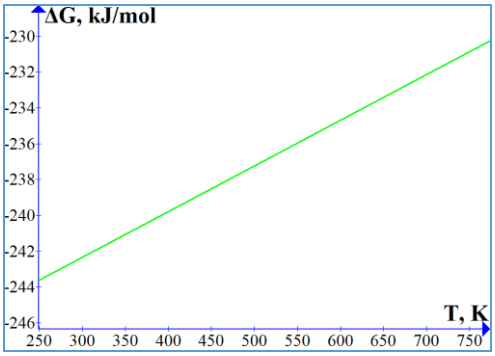

Fig. 3: Temperature dependence of the Gibbs free energy change for the reaction.

The Gibbs free energy profile of the reaction demonstrates that the process remains spontaneous throughout the entire practically relevant temperature range. Although the ΔG value shows a slight increase with rising temperature, the magnitude of this change is relatively small and does not substantially influence the thermodynamic feasibility of the reaction. Consequently, performing the reaction in acetonitrile medium within the 323–343 K temperature interval may be regarded as thermodynamically and kinetically favourable. Under these conditions, the SN2 substitution process proceeds more rapidly, while the physicochemical characteristics of the solvent provide an appropriate environment for efficient nucleophilic attack and stabilisation of the reaction system, thereby promoting effective formation of the desired product.

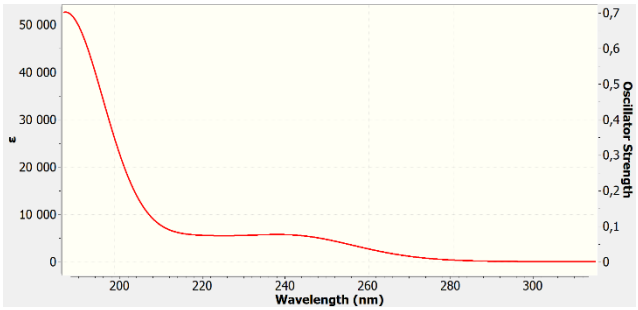

Fig. 4: TD-DFT simulated UV–Vis spectrum of 3-(1,3-dihydroxypropan-2-yl)benzo[*d*]oxazol-2(3*H*)-one.

The electronic characteristics of 3-(1,3-dihydroxypropan-2-yl)benzo[*d*]oxazol-2(3*H*)-one were analysed using UV–Vis spectroscop-ic calculations together with frontier molecular orbital (HOMO–LUMO) analysis. The computational results confirmed the existence of an extended conjugated electronic system within the molecule and demonstrated that the observed electronic transitions predominantly originate from the aromatic ring and carbonyl-containing fragments.

The TD-DFT calculations predicted the main absorption bands at approximately 190 nm and 243.8 nm (Figure 4). The strong absorption band near 190 nm is attributed to high-energy π→π* transitions occurring mainly within the aromatic π-conjugated system of the benzoxazolinone framework. The considerable intensity of this band indicates efficient delocalisation of π-electrons across the molecular structure.

The absorption maximum around 243.8 nm corresponds to lower-energy electronic excitations and is mainly associated with n→π* transitions, together with partially overlapping π→π* transitions involving the carbonyl functionality and heteroatom lone-pair electrons. In particular, the nonbonding electron pairs located on the nitrogen and oxygen atoms make a substantial contribution to the formation of the HOMO orbital and strongly influence the electronic excitation behaviour of the molecule.

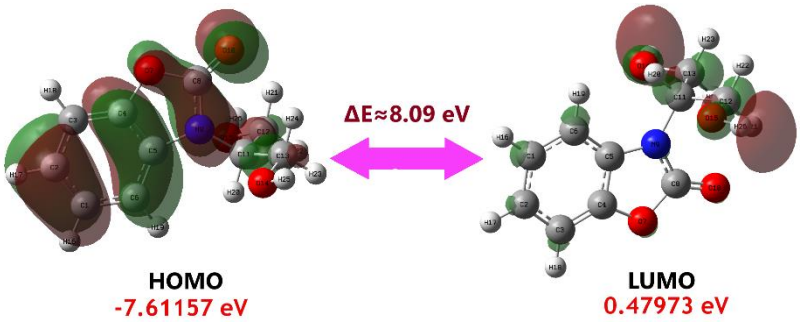

Fig. 5: Spatial distribution of the HOMO and LUMO orbitals with the calculated energy gap (Δ*E* ≈ 8.09 eV).

The frontier molecular orbital calculations revealed that the HOMO energy of the studied molecule is −0.27972 a.u. (−7.61157 eV), while the LUMO energy is 0.01763 a.u. (0.47973 eV) (Figure 5). Based on these values, the HOMO–LUMO energy separation was estimated to be approximately 8.09 eV. Such a relatively large energy gap suggests that the molecule possesses considerable kinetic stability and requires a relatively high excitation energy for electronic transitions. This observation is in good agreement with the UV–Vis spectral data, where the principal absorption bands are located predominantly in the ultraviolet region.

Analysis of the orbital distributions showed that the HOMO is mainly concentrated over the aromatic ring system, the nitrogen atom, and partially the hydroxyl substituents, indicating that these regions represent the electron-donating part of the molecule. In contrast, the LUMO is primarily localised on the carbonyl group and the antibonding π* orbitals of the heterocyclic fragment, identifying these regions as electron-accepting centres. Consequently, upon electronic excitation, electron density is transferred from the HOMO toward the LUMO, resulting in intramolecular charge transfer within the molecular framework.

Accordingly, the absorption band observed near 243.8 nm in the UV–Vis spectrum can be assigned mainly to HOMO→LUMO electronic excitation. This transition is associated with the migration of electron density from the lone-pair orbitals of the nitrogen and oxygen atoms toward the antibonding orbitals of the carbonyl fragment. The Mulliken charge distribution results further support this interpretation, since the nitrogen atom carries a pronounced negative charge ($q_N \approx -0.459$), whereas the carbonyl carbon atom exhibits a considerable positive charge ($q_C \approx +0.454$).

Overall, the combined UV–Vis spectral analysis and HOMO–LUMO investigation confirm the existence of extensive electron delo-calisation within the molecule. The calculated transitions are predominantly characterised by π→π* and n→π* excitation processes, while the large HOMO–LUMO energy gap indicates substantial electronic and thermodynamic stability of the benzoxazolinone-based system.

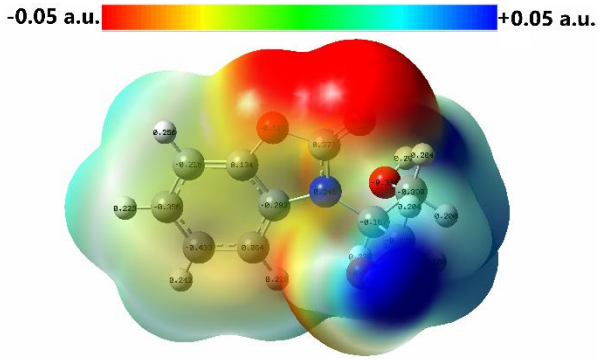

Fig. 6: Molecular electrostatic potential (MEP) map of 3-(1,3-dihydroxypropan-2-yl)benzo[*d*]oxazol-2(3*H*)-one.

The molecular electrostatic potential (MEP) surface provides a clear visualisation of the electron density distribution within the 3-(1,3-dihydroxypropan-2-yl)benzo[*d*]oxazol-2(3*H*)-one molecule (Figure 6). This analysis enables identification of the molecular regions most prone to electrophilic and nucleophilic interactions and further supports the results obtained from Mulliken charge calculations, frontier molecular orbital analysis, and UV–Vis spectral investigations.

In the MEP representation, red-colored regions correspond to zones of high electron density and negative electrostatic potential, whereas blue regions indicate electron-deficient areas characterised by positive electrostatic potential. Intermediate electron density is represented by green and yellow colours.

The most pronounced negative electrostatic potential is localised around the carbonyl oxygen atom and the hydroxyl oxygen atoms. The intense red colouration in these regions reflects substantial electron accumulation, indicating that these atoms constitute the most electron-rich centres of the molecule. In particular, the carbonyl oxygen atom exhibits especially strong electron density, which is fully consistent with the Mulliken population analysis showing a significant negative atomic charge on this atom. The elevated electron density surrounding the oxygen atoms enhances their capability to participate in hydrogen-bond formation and interactions with electrophilic species.

Conversely, the blue-colored regions are primarily concentrated around the hydrogen atoms of the hydroxyl groups. These regions possess relatively low electron density and positive electrostatic potential, indicating their susceptibility to intermolecular hydrogen-bond interactions. Such polarisation of the O–H bonds contributes to the intermolecular interaction ability of the molecule in polar environments.

The green–yellow electrostatic potential distribution over the aromatic benzoxazolinone framework suggests considerable delocalisation of electron density

throughout the conjugated system. This observation agrees well with the frontier molecular orbital analysis, where the HOMO orbital was found to be localised mainly over the aromatic ring and nitrogen atom, enhancing the electron-donating character of these fragments. At the same time, localisation of the LUMO orbital around the carbonyl-containing region supports the occurrence of intramolecular charge-transfer processes.

The MEP analysis is also in good agreement with the calculated UV–Vis spectral properties. In particular, the absorption band near 243.8 nm can be associated with electron-density transfer from donor regions toward electron-accepting fragments of the molecule. In this process, the nitrogen and oxygen atoms function as electron donors, whereas the carbonyl group acts predominantly as an electron-accepting centre.

Overall, the molecular electrostatic potential map confirms the highly non-uniform nature of electron density distribution in the molecule and demonstrates the presence of significant electron delocalisation within the benzoxazolinone system. The obtained results are fully consistent with the Mulliken charge analysis, HOMO–LUMO calculations, and UV–Vis spectral data, providing a comprehensive interpretation of the electronic structure, stability, and reactivity of the studied compound.

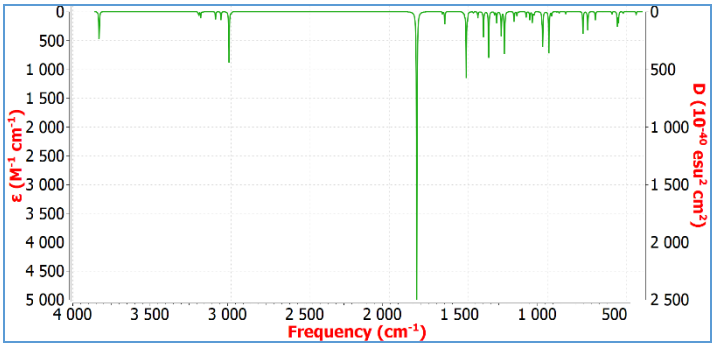

Fig. 7: Calculated FTIR spectrum of 3-(1,3-dihydroxypropan-2-yl)benzo[*d*]oxazol-2(3*H*)-one.

The principal absorption bands observed in the calculated FTIR spectrum successfully confirm the presence of the functional groups in 3-(1,3-dihydroxypropan-2-yl)benzo[*d*]oxazol-2(3*H*)-one (Figure 7).

The weak but relatively intense peaks observed around 3831–3833 cm^{-1} correspond to the stretching vibrations of free or weakly hydrogen-bonded O–H groups. Since the molecule contains two alcoholic hydroxyl groups, the presence of these signals is expected. In experimental spectra, the O–H absorption band is usually

broader; however, in the calculated FTIR spectrum it appears as a narrow and sharp peak.

The peaks located within the 3176–3208 cm^{-1} region are associated with vibrations involving aromatic and heterocyclic C–H bonds as well as partially N–C-related vibrations. Hydrogen-bonded O–H components may also contribute to this region to some extent.

The absorption bands at 2997–3011 cm^{-1} correspond to the C–H stretching vibrations of aliphatic CH_2 groups, confirming the pres-ence of $–CH_2OH$ fragments in the side chain. The signals observed within the 3060–3096 cm^{-1} range are characteristic of aromatic ring C–H stretching vibrations.

The strong absorption peak at 1824 cm^{-1} is characteristic of the ν(C=O) stretching vibration of the carbonyl group. This clearly confirms the presence of the cyclic carbonyl group of the benzoxazolinone system. The relatively high frequency of this vibration is associated with the incorporation of the carbonyl group within the heterocyclic system as well as with resonance and inductive effects.

The band at 1647 cm^{-1} corresponds to a mixed region involving conjugated C=C and ring C–N vibrations. The strong absorption peak at 1511 cm^{-1} is related to aromatic ring skeletal vibrations together with the C–N resonance system. The bands observed within the 1369–1402 cm^{-1} range are attributed to CH_2 deformation vibrations and C–N stretching components. The very strong signal at 1269 cm^{-1} is highly characteristic of Ar–O–C and C–O stretching vibrations, confirming the presence of the ether-like bond within the benzoxazole ring. The intense absorption bands observed in the 1027–1109 cm^{-1} region correspond to C–O stretching vibrations of alcohol groups and are in very good agreement with the presence of two hydroxymethyl fragments in the molecule.

The bands observed at 743 and 773 cm^{-1} correspond to out-of-plane C–H vibrations of the aromatic ring and indicate the substitut-ed nature of the benzene ring.

Overall, the calculated FTIR spectrum confirms the presence of hydroxyl groups (O–H), a cyclic carbonyl group (C=O), an aromatic ring system, and C–O as well as C–N bonds, and is therefore in excellent agreement with the proposed molecular structure.

When the reducing and electron-donating properties of 3-(1,3-dihydroxypropan-2-yl)benzo[*d*]oxazol-2(3*H*)-one are evaluated on the basis of all quantum-chemical results — including Mulliken charge distribution, Fukui function analysis, HOMO–LUMO calcu-lations, MEP mapping, and UV–Vis spectral data — the molecule can be characterized as a system possessing local electron-donating centers while

exhibiting relatively high overall kinetic stability and moderate electron-donating ability.

According to the Mulliken charge distribution analysis, a large negative charge (−0.459) is localized on the nitrogen atom of the benzoxazolinone fragment. A significant negative charge (−0.381) was also observed on the carbonyl oxygen atom.

These values indicate high electron density on the nitrogen and oxygen atoms and demonstrate that these centers actively participate as electron donors. In particular, the resonance delocalization of the lone electron pair of the nitrogen atom over the aromatic and carbonyl system suggests the presence of strong electron migration within the molecule. The results of the Fukui function analysis further support this conclusion (Table 2). According to the orbital-weighted condensed Fukui indices, the highest value (f^- = 0.09961) was observed for the nitrogen atom. In addition, the dual descriptor value (Δf) of −0.09405 indicates that the nitrogen atom acts as a strong nucleophilic and electron-donating center. The carbonyl oxygen atom also exhibits a high f^- value, confirming the presence of several electron-donating centers within the molecule [15, 16].

Table 2: Orbital-weighted condensed Fukui function indices and dual descriptor values for 3-(1,3-dihydroxypropan-2-yl)benzo[*d*]oxazol-2(3*H*)-one

Atom index	OWf^+	OWf^-	OWf^0	OW DD
C1	0.03108	0.09358	0.06233	-0.06250
C2	0.03125	0.11668	0.07396	-0.08543
C3	0.03590	0.07251	0.05420	-0.03662
C4	0.02601	0.10376	0.06489	-0.07775
C5	0.02060	0.09946	0.06003	-0.07886
C6	0.03228	0.08925	0.06077	-0.05697
O7	0.01243	0.03965	0.02604	-0.02721
C8	0.02652	0.03326	0.02989	-0.00674
N9	0.00556	0.09961	0.05258	-0.09405
O10	0.01790	0.08694	0.05242	-0.06904
C11	0.00410	0.01324	0.00867	-0.00915
C12	0.01149	0.01489	0.01319	-0.00340
C13	0.01149	0.01489	0.01319	-0.00341
O14	0.01060	0.03272	0.02166	-0.02211
O15	0.01061	0.03272	0.02166	-0.02211
H16	0.03820	0.00800	0.02310	0.03020
H17	0.03807	0.01060	0.02434	0.02748
H18	0.04094	0.00536	0.02315	0.03558
H19	0.02829	0.00681	0.01755	0.02147
H20	0.01338	0.00168	0.00753	0.01170

H21	0.02228	0.00434	0.01331	0.01794
H22	0.03015	0.00532	0.01773	0.02483
H23	0.03015	0.00532	0.01774	0.02483
H24	0.02228	0.00434	0.01331	0.01794
H25	0.05032	0.00256	0.02644	0.04776
H26	0.05033	0.00256	0.02645	0.04777
Sum of orbital weighted f^+			Sum of orbital weighted f^-	
0.652196			1.000037	

The presence of negative dual descriptor values throughout the aromatic system further confirms the delocalized nature of the π-electrons. This indicates the existence of intramolecular charge transfer processes within the molecule.

According to the frontier molecular orbital analysis, the HOMO orbital is mainly localized over the nitrogen atom, the aromatic ben-zoxazolinone nucleus, and partially over the hydroxyl fragments. This demonstrates that these fragments constitute the electron-donating part of the molecule. The HOMO energy value was calculated to be −7.61 eV, indicating the presence of electron-donating ability within the molecule. However, since this value is not particularly high, the compound cannot be regarded as a strong reducing agent, but rather as a moderate electron donor. In contrast, the LUMO orbital is mainly localized over the carbonyl fragment and the antibonding π* orbitals. The HOMO→LUMO electron migration indicates the occurrence of donor–acceptor type electron trans-fer within the molecule. As discussed above, the HOMO–LUMO energy gap was found to be 8.09 eV. This relatively large energy gap indicates considerable kinetic stability and suggests that a significant amount of energy is required for electron transfer to an external system. Therefore, the reducing ability of the compound is limited, although its local donor centers are clearly pronounced.

The MEP map also demonstrates the presence of electron-donating centers within the molecule. The red regions of the map are mainly localized around the carbonyl oxygen atom and the hydroxyl oxygen atoms, confirming the high electron density on these atoms. These centers can readily interact with electrophilic reagents and participate in hydrogen-bond formation. Furthermore, due to the presence of hydroxyl and heteroatom-containing fragments, the molecule may also exhibit potential antioxidant and redox-active properties.

CONCLUSION

In this study, the electronic structure, thermodynamic stability, and spectral properties of 3-(1,3-dihydroxypropan-2-yl)benzo[*d*]oxazol-2(3*H*)-one were investigated using DFT and TD-DFT methods at the B3LYP/6-311G(d,p) level in

acetonitrile medium. The obtained results demonstrated good agreement between Mulliken charge analysis, Fukui function calculations, HOMO–LUMO analysis, MEP mapping, UV–Vis, and FTIR spectra.

The calculations confirmed that the nitrogen and oxygen atoms act as the principal electron-donating and nucleophilic centers of the molecule, supporting the proposed SN2 reaction mechanism. The HOMO–LUMO energy gap of approximately 8.09 eV indicated considerable kinetic stability, while the negative Gibbs free energy values confirmed the thermodynamic favorability and spontaneous character of the reaction. The investigated benzoxazolinone derivative was found to possess moderate electron-donating and reducing properties together with strong electron delocalization and structural stability.

REFERENCES

[1] Joule JA, Mills K (2010), Heterocyclic Chemistry, 5th edn. Wiley-Blackwell, Oxford, pp: 1–720.

[2] Katritzky AR, Ramsden CA, Scriven EFV & Taylor RJK (2008), Comprehensive Heterocyclic Chemistry III. Elsevier, Amsterdam, pp: 1–12560.

[3] Kakkar S & Narasimhan B (2019), A comprehensive review on biological activities of oxazole derivatives. BMC Chemistry 13, pp:16–16.

[4] Cramer CJ (2013), Essentials of Computational Chemistry: Theories and Models, 2nd edn. Wiley, Chichester, pp:1–596.

[5] Becke AD (1993), Density-functional thermochemistry. III. The role of exact exchange. Journal of Chemical Physics 98, pp:5648–5652.

[6] Lee C, Yang W & Parr RG (1988), Development of the Colle–Salvetti correlation-energy formula into a functional of the electron density. Physical Review B 37, pp:785–789.

[7] Mulliken RS (1955), Electronic population analysis on LCAO–MO molecular wave functions. Journal of Chemical Physics 23, pp:1833–1840.

[8] Carey FA & Sundberg RJ (2007), Advanced Organic Chemistry. Part A: Structure and Mechanisms, 5th edn. Springer, New York, pp: 1–1196.

[9] Anslyn EV & Dougherty DA (2006), Modern Physical Organic Chemistry. University Science Books, Sausalito, pp:1–1104.

[10] Reichardt C & Welton T (2011), Solvents and Solvent Effects in Organic Chemistry, 4th edn. Wiley-VCH, Weinheim, pp:1–718.

[11] Frisch MJ et al. (2013), Gaussian 09 Revision D.01. Gaussian Inc., Wallingford CT.

[12] Silverstein RM, Webster FX, Kiemle DJ & Bryce DL (2014), Spectrometric Identification of Organic Compounds, 8th edn. Wiley, Hoboken, pp:1–464.

[13] Stiti M, Bouzit H, Boudjahem AG, Cheghib N, Derdare M & Ksouri R (2025), Experimental and theoretical studies on the inclusion process of the benzoxazolinone in β-cyclodextrin. Russian Journal of Physical Chemistry A 99, pp:237–249.

[14] Syetov Y (2026), Calculations of infrared spectra of benzoxazoles exhibiting excited-state proton transfer by a composite method. Ukrainian Journal of Physical Optics 27, pp:02035–02042.

[15] Allison TC & Tong YJ (2013), Application of the condensed Fukui function to predict reactivity in core–shell transition metal nanoparticles. Electrochimica Acta 101, pp:334–340.

[16] Faver J & Merz KM Jr (2010), Utility of the hard/soft acid–base principle via the Fukui function in biological systems. Journal of Chemical Theory and Computation 6, pp:548–559.